

High Frame Rate Measurement of Two-Dimensional Heart Wall Motion for Assessment of Regional Myocardial Contraction and Relaxation

局所心筋収縮弛緩特性計測のための2次元心臓壁運動の高フレームレート計測

Yasunori Honjo^{1†}, Hideyuki Hasegawa^{1,2} and Hiroshi Kanai^{2,1} (¹Graduate School of Biomedical Eng., Tohoku Univ.; ²Graduate School of Eng., Tohoku Univ.)
本庄 泰徳^{1‡}, 長谷川 英之^{1,2}, 金井 浩^{2,1} (¹東北大学医工; ²東北大学工)

1. Introduction

For noninvasive and quantitative measurement of global two-dimensional (2-D) heart wall motion, speckle tracking methods have been applied¹⁾. However, an important parameter, the optimal size of a correlation kernel, has not been thoroughly investigated. Moreover, the frame rate in these methods is limited to about 200 Hz, corresponding to the sampling period of 5 ms. Under rapid motion of the heart, speckle tracking methods may fail to estimate the heart wall motion at a low frame rate because it leads to significant changes in echo patterns. In our previous study, the optimal kernel size was determined in a phantom experiment and, then, the determined optimal kernel size was applied to the *in vivo* experiment of 2-D velocities of the heart wall by normalized cross-correlation between RF echoes²⁾. However, evaluation for measurement of the strain rate is not sufficient.

In the present study, the determined kernel size was applied for calculating the strain rate and compared with other sizes and then, myocardial strain rate was measured so that the myocardial function could be measured at a high frame rate.

2. Principle

2.1 Definition on Correlation Kernel

As illustrated in Fig. 1, the sizes of the correlation kernel in the lateral direction W_l and that in the axial direction W_d were defined using the widths $\Delta l(d)$ and $\Delta d(d)$ at half maxima of the lateral profile of an ultrasonic field and the envelope of an ultrasonic pulse at each depth d .²⁾

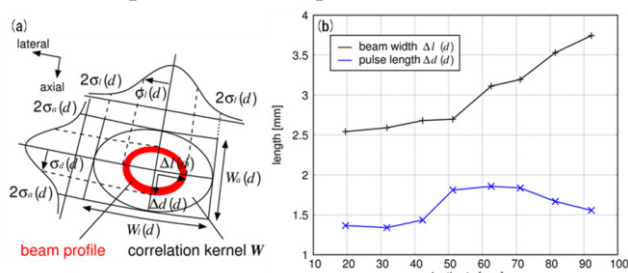


Fig. 1: (a) Schematic of correlation kernel ($W_l \times W_d$).

(b) Estimated beam wide Δl and pulse length Δd .

2.2 Calculation of the Radial Strain Rate

We introduced the strain rate to evaluate how the thickness of layer changes with respect to time. As shown in Fig. 2(a), the velocities $v_r(\theta_i, j; n)$ in the radial direction are given by

$$v_r(\theta_i, j; n) = v_l(l, d; n) \cdot \sin(\theta_i + \theta(l)) + v_a(l, d; n) \cdot \cos(\theta_i + \theta(l)) \quad [\text{m/s}], \quad (1)$$

where $v_l(l, d; n)$ and $v_a(l, d; n)$ are the velocities in the lateral and axial directions at lateral position l and depth d , respectively. As shown in Fig. 2(b), strain rate in the radial direction, $S_r(\theta_i, j; n)$, between j -th and $(j+1)$ -th layer are given by

$$S_r(\theta_i, j; n) = \frac{v_r(\theta_i, j+1; n) - v_r(\theta_i, j; n)}{L} \quad [(\text{m/s})/\text{m}]. \quad (2)$$

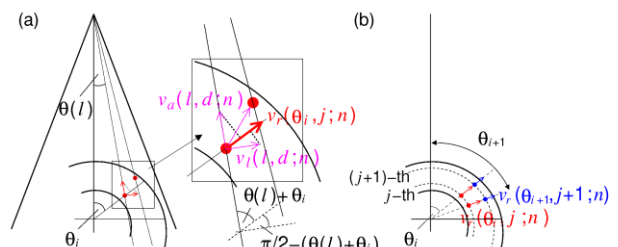


Fig. 2: Schematic of calculation of radial strain rate.

3. Basic Experiment

3.1 Experimental System

As illustrated in Fig. 3, in this experiment, strain rate of a phantom due to the change in the internal pressure, which was applied by a flow pump, was measured. The homogeneous cylindrical phantom was made from silicone rubber whose thickness was 2 mm. RF data were acquired using a 3.75 MHz sector-type probe of ultrasonic diagnostic equipment (Aloka α -10). The sampling frequency of the RF signal was 15 MHz. The frame rate and angular interval of beams $\delta\theta$ were 860 Hz and 0.375 degrees, respectively.

In this study, to obtain the actual velocity $v_{r0}(\theta_i, j; n)$ and strain rate $S_{r0}(\theta_i, j; n)$, 1-D phased sensitive method³⁾ (1-D method) was used for the phantom at the central beam ($\theta_i = 0$ [deg]). The silicone rubber assumed to be isotropic medium. Therefore, radial

strain rate $S_r(\theta_i, j; n)$ at θ_i between j -th and $(j+1)$ -th layer, equals to the strain rate $S_{r0}(\theta_i, j; n)$ ($\theta_i = 0$ [deg]) obtained by 1-D method.

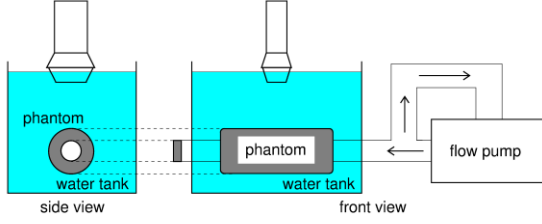


Fig. 3: Schematic of system for basic experiment.

3.3 Experimental Result

To compare the optimal size of kernel, which determined in a phantom experiment²⁾, with other sizes^{1, 4)}, the radial strain rates estimated using different kernel sizes were examined using the normalized mean-squared error (MSE) of the estimated strain rate from the actual strain rate. The normalized mean-squared error $\varepsilon(\theta_i)$ was calculated from the radial strain rate $S_r(\theta_i, j; n)$ for each position (θ_i, j) and actual $S_{r0}(\theta_i, j; n)$ as follows:

$$\varepsilon(\theta_i) = \frac{\sum_{j=0}^{J-1} \sum_{n=0}^{N-1} (S_r(\theta_i, j; n) - S_{r0}(\theta_i, j; n))^2}{\sum_{j=0}^{J-1} \sum_{n=0}^{N-1} (S_{r0}(\theta_i, j; n))^2}, \quad (3)$$

where J and N are the number of layers and the number of frames, respectively.

Figure 4 shows the distribution of MSE, $\varepsilon(\theta_i)$, estimated using different sizes of the correlation kernels, $(4.0 \times 4.0) \text{ mm}^1$, $(11.6 \times 6.4) \text{ mm}^2$ and $(10 \times 10) \text{ mm}^4$. The strain rates in the radial directions with the correlation kernel size of $(11.6 \times 6.4) \text{ mm}^2$ yielded the least MSE. On the other hand, the strain rate estimated using the previously examined kernel sizes, $(4.0 \times 4.0) \text{ mm}^1$ and $(10 \times 10) \text{ mm}^4$, were markedly different from the actual one. Compared with conventional kernel sizes, this result shows the possibility of the proposed correlation kernel $(11.4 \times 6.4) \text{ mm}$ for more accurate measurement of the strain rate.

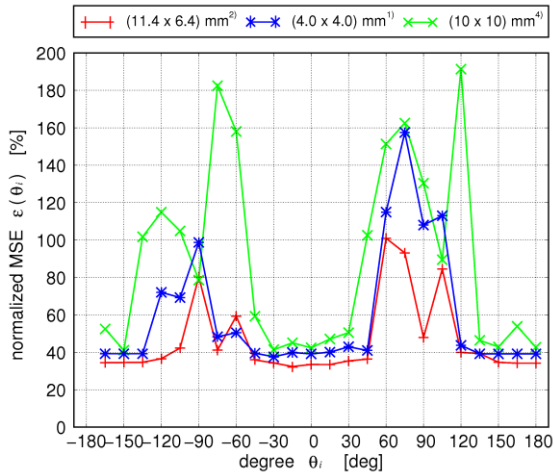


Fig. 4: Distribution of MSE $\varepsilon(\theta_i)$

4. In Vivo Experimental Results

As shown in Fig. 5, strain rate in a region in the IVS (56 yellow points in Fig. 5(a)) were estimated by 2-D tracking. The size of a correlation kernel was set at $(11.4 \times 6.4) \text{ mm}^2$. Figures 5(c) and 5(d) show the distribution of strain rates at every 2 ms in the radial and longitudinal directions at the beginning of the second heart sounds, respectively. The transition from contraction to relaxation was not uniform at each position, and the basal side relaxes earlier than the apical side. The strain rate in the radial direction is perpendicular to that in the longitudinal direction. Therefore, myocardial contraction and relaxation (in the longitudinal direction) in the IVS correspond to increase and decrease in thickness in the radial direction, respectively³⁾. This phenomenon of strain rates obtained by 2-D tracking was in good agreement with those relationships.

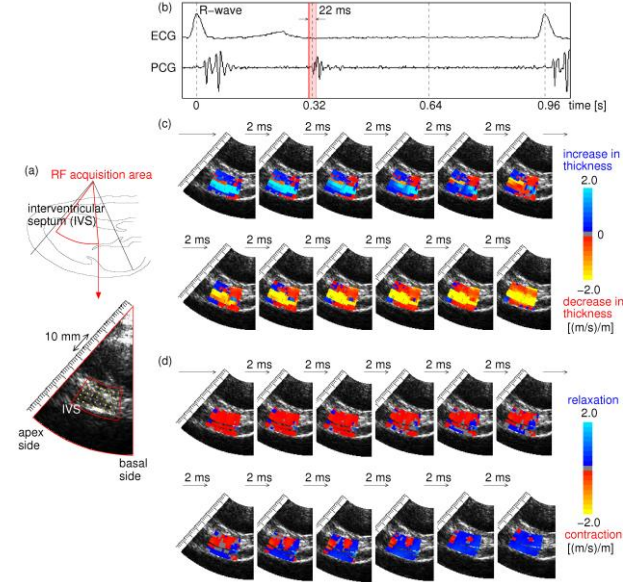


Fig. 5: (a) Acquisition area of the RF echoes from the longitudinal-axis view. Distributions of the strain rate around the second heart sound in the axial (c) and lateral (d) directions.

5. Conclusion

Myocardial strain rates were measured at a high temporal resolution. As shown in Fig. 5, *in vivo* experimental results show the possibility of this method for measurement of 2-D heart motion to assess the regional myocardial contraction and relaxation at a high temporal resolution.

References

1. J. D'hooge, *et al.*: IEEE Trans. UFFC **49** (2002) 281.
2. Y. Honjo, *et al.*: IEICE. J94 **11** (2011) (in japanese) (in press).
3. H. Kanai, *et al.*: Jpn. J. Appl. Phys. **38** (1999) 3403.
4. S. Nakatani: GE today, July 2003.